

3D full wave code modelling of ECRF plasma heating in tokamaks and ITER at fundamental and second harmonics

Vdovin V.L.

RRC Kurchatov Institute Tokamak Physics Institute

vdov@nfi.kiae.ru

Abstract We present recent numerically well resolved 3D ECRF STELEC full wave code modelling results for fundamental and second harmonics scenarios in tokamaks and ITER. STELEC code is now updated and includes also non diagonal wave induced plasma current response terms important for quasi perpendicular O-mode launch. The modelled are ECH scenarios for operating T-10, DIII-D, JET and TCV machines. Improved numerical resolution for these middle size tokamaks further solidly confirms previously discovered O- and X- modes strong coupling at fundamental harmonic leading to broadened power deposition profiles, in compare with ray tracing predictions, due to influence of Upper Hybrid Resonance (UHR). For the T-10 tokamak we consider O-mode outside launch cases with EC resonance in plasma with UHR usual “mirror like” surface and out off plasma fundamental harmonic EC resonance at High Field Side when UHR surface is in-plasma internally closed one with the Electron Bernstein Waves (EBW) being excited inside of it due to mode conversion process. Combined self consistent dynamic O-mode, X-mode and EB waves structure in toroidal plasma is intriguing one and is demonstrated. At this last scenario firstly discovered in WEGA stellarator with quasi perpendicular outside launch the waves are absorbed at the second harmonic – due to relativity effects. O-X-B scenario modelling results for several tokamaks are also given. Implications for the ITER are given strongly showing re evaluation need for the ECH NTM stabilization concept. In second harmonic scenarios we concentrate on X-mode outside launch at sufficiently large plasma densities, some times close (but lower) to this mode density cut off. Exact solution again shows that simultaneously the O-mode is also excited (with smaller amplitude), presumably due to reflection effects and wave depolarization at the wall. High densities regimes are interesting ones because inside of plasma may be created two power deposition peaks. Examples for T-10 and JET are given. ITER second harmonic scenario for non active plasma phase at half magnetic field was also explored.

1. Fundamental harmonic modeling

1.1 Out of plasma EC resonance scenario

ECH out of plasma fundamental resonance O-mode launch high resolution modelling at low frequency strongly validates that EBWs play crucial role in toroidal plasmas. Unusual scenario with out of plasma cold electron fundamental cyclotron resonance at HFS in the WEGA stellarator has shown [2] the efficient ECRF heating with two groups heated electrons: fast electrons group and warm electrons. Our idea was that main heating role play Electron Bernstein Waves born at Upper Hybrid Resonance and well trapped in core plasma. FIG.1 shows O-X-B eigen modes coupling at EC resonance out off plasma fundamental harmonic in DIII-D/WEGA-like oblique $N_{\parallel}=0.32$ O-mode outside launch with $F=6$ GHz, $B_0=0.16$ T, $N_e(0)=2.3 \cdot 10^{17} \text{ m}^{-3}$, $T_e(0)=9.2\text{kV}$ at $N_e(0) < N_{\text{crit}|O-mode}$. The Mode Converted EB Waves are shown by red colour in expanded scale in FIG.1b. The X-mode, experiencing its density cut off, appears automatically, presumably due to plasma toroidicity, wave reflection and O- and X-mode coupling through the boundary conditions at the conducting wall surrounding plasma.

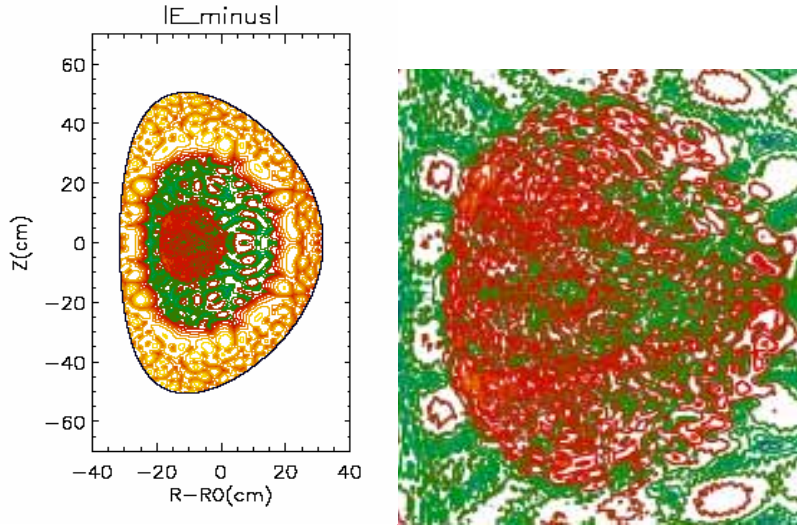


FIG 1a,b. Contour plots of $|E_minus|$ e.m. (yellow-green) and EB Waves (red) at 6 GHz for DIII-D/Wega-like scenario. Oblique O-mode outside launch, $N_{||}=0.32$

Radial power deposition profile for this DIII-D/WEGA-like scenario is given in FIG.2 with power absorption at second and fundamental harmonics: $P_e(2\omega_{ce}) = 61\%$ (red), $P_e(\omega_{ce}) = 39\%$. The O-X-B modes coupling at EC out off plasma fundamental harmonic in T-10-like **O-mode quasi perpendicular** $N_{||}=0.016$ outside launch at $N_e < N_{crit|O-mode}$ $|E_minus|$ is displayed in FIG.3 and shows O-, X-mode and EB waves interplay. Power in this scenario is mainly absorbed at the second harmonic due to relativistic effects.

1.2 DIII-D/T-10 fundamental harmonic modelling at 60 GHz

Similar EC heating efficiencies at fundamental harmonic in DIII-D for O-mode and X-mode outside launches at 60 GHz were reported [3,4]. Their nice explanation

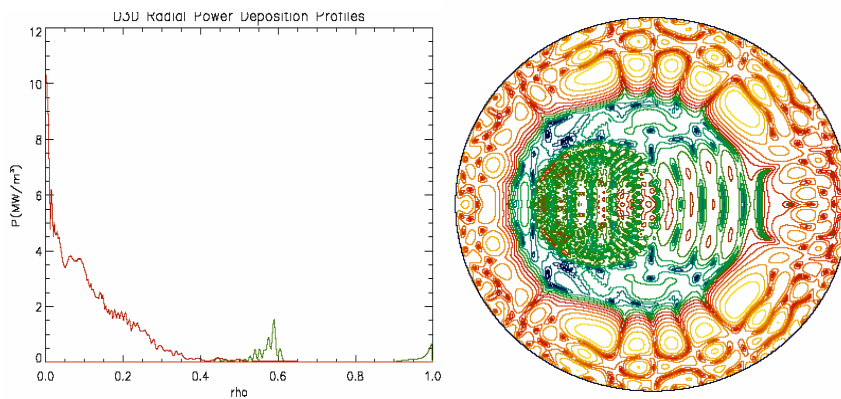
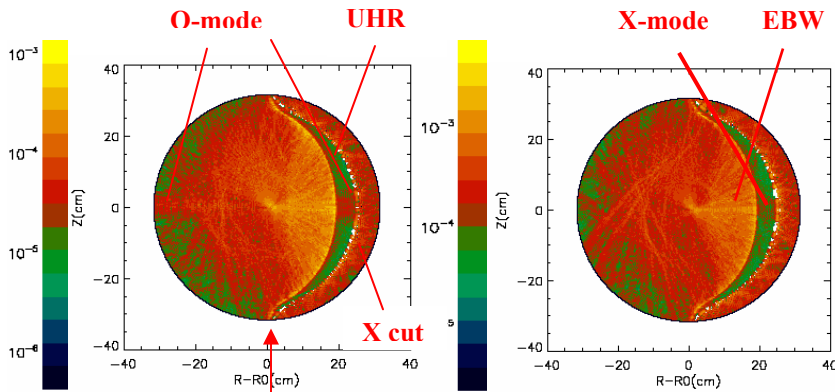


FIG. 2 Radial power deposition, $N_{||}=0.3$. FIG.3 $|E_|$ in T-10-like at $N_{||}=0.016$

argued to X-mode reflection from the X's cut off and conversion to the O-mode during reflection from the walls. STELEC code treats this effect automatically. Modelling was performed for O- and X-mode antenna polarizations at $F=60$ GHz, $B_o=2.14$ T, $I_p=0.14-0.28$ MA, $N_e(0)=2.3 \cdot 10^{19} \text{ m}^{-3}$, $N_e(s)=2.3 \cdot 10^{18} \text{ m}^{-3}$, $\alpha_n=1.0$, $T_e(0)=36.8\text{kV}$ (to increase EBW resolution), $\alpha_T=2.0$, outside launch spectrum $N_{//}(0)=0.016 - 0.3$, RF power 1 MW. FIG.4 displays $|E_{\psi}|$ contour plots for O- launch (left) and X-mode launch (right) in T-10/DIII-D at $N_{//}=0.16$. One sees the X-mode appearance (with its cut off), even at O-mode antenna polarization, the UH resonance broadly borrows the EBW. Both scenarios look similar ones but waves amplitudes for X-antenna are remarkably higher ones: $A(\text{X-mode}) \sim 7A(\text{O-mode})$ – as it is predicted by WKB (rays) treatment due to weaker X-mode attenuation.



$$\Omega = \omega_{ce}$$

FIG.4a Radial field $|E_{\psi}|$ for O-mode antenna. FIG.4b $|E_{\psi}|$ for X-mode antenna.

Radial power deposition profiles for both cases are shown in FIGs.5a,b.

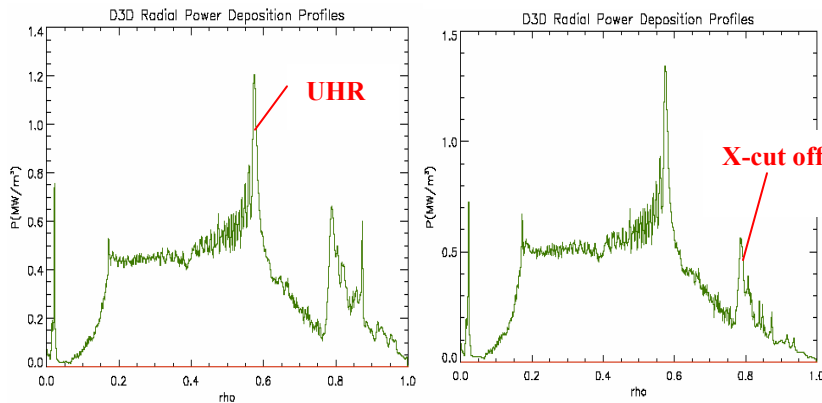


FIG.5a Power deposition for O-antenna, $N_{//}=0.16$ FIG.5b Power deposition for X-antenna

Power deposition for O- and X-mode in T10/DIII-D at 60 GHz at quasi perpendicular launch $N_{//}=0.016$ are again very similar while X-mode excited amplitudes are ~ 10 times higher of O-mode case (FIGs.6a,b). This modelling strongly supports very similar

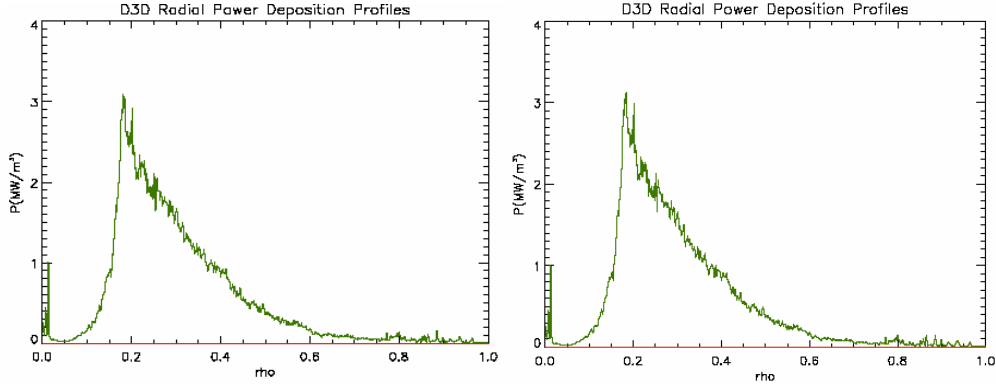


FIG.6a Power deposition for O-antenna, $N_{//}=0.016$ FIG.6b Power deposition for X-antenna

heating efficiencies and temperature profiles reported by DIII-D [3,4] for both antenna polarizations thus confirming O- and X-modes coupling in toroidal plasma.

ITER fundamental harmonic modelling was performed reduced at reduced frequency 11.15 GHz due to lack of adequate world Super Computer to model so large scale plasma at specified 170 GHz . This approach makes use the similarity laws formulated in [1]. Machine and plasma parameters were: $B_0=0.33-0.39$ T, $I_p=0.634$ MA, $N_e(0)=3 \cdot 10^{17} \text{ m}^{-3}$, $N_e(s)=3 \cdot 10^{16} \text{ m}^{-3}$, $\alpha_n=1.0$, $T_e(0)=25.8\text{kV}$, $\alpha_T=1.0$, outside launch spectrum $N_{//}(0)=0.016 - 0.5$, RF power 1 MW. The O-mode fundamental harmonic quasi perpendicular equatorial launch at $N_{//}=0.017$, $B_0=0.381$ T, is demonstrated by $|\text{Re}(E_{\text{minus}})|$ contour plots in FIG.7 and power deposition in FIG.8. The EC and UHR resonances positions in equatorial plane are $X(\omega_{ce})= -27$ cm, $X(\text{UHR})=38$ cm.

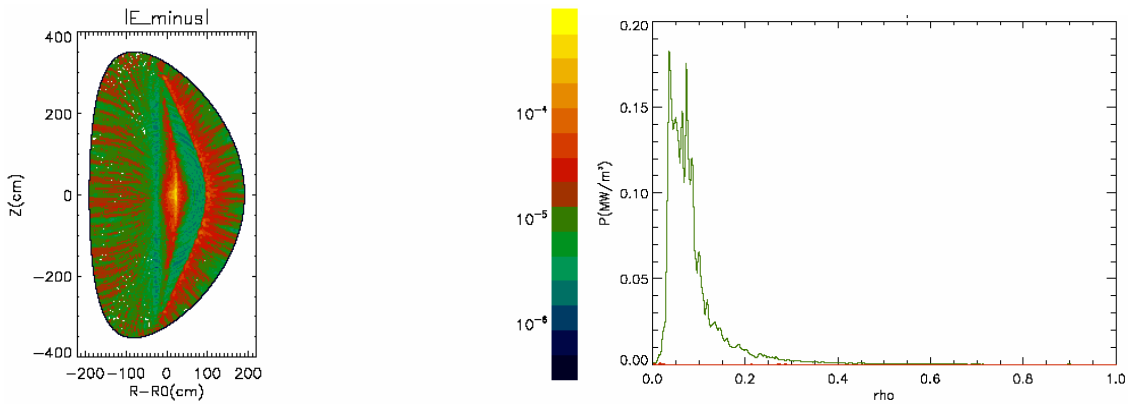


FIG.7 $|\text{Re}(E_{\text{minus}})|$ in ITER at $N_{//}=0.017$ FIG.8 Power deposition in ITER at $N_{//}=0.017$

The $|\text{Im}(E_z)|$ field contour plots and radial power deposition $P(\rho)$ at O-mode fundamental harmonic oblique equatorial launch at $N_{//}=0.49$, at increased $B_0=0.391$ T with $X(\omega_{ce})= -11$ cm, $X(\text{UHR})=53.5$ cm, are given by FIGs.9,10.

For both cases we see that power deposition is governing by UHR position, large amplitudes small scale EBW activity near of it. Important to stress that EBW are interacting with small group of very energetic electrons which can contribute to highly localised and efficient Current Drive, e.g. for NTM suppression.

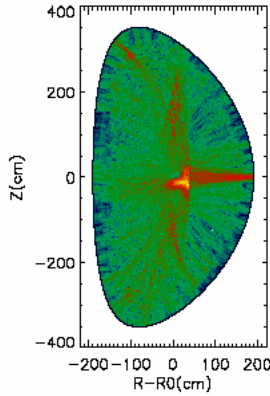


FIG. 9 $|Im(E_z)|$ in ITER at $N_{\parallel}=0.49$

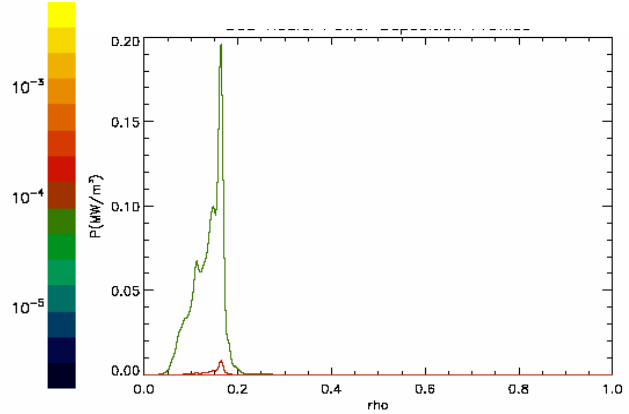


FIG.10 power deposition $P(r)$ in ITER at $N_{\parallel}=0.49$

2. Second harmonic ECRF modelling

There are no Upper Hybrid resonance at typical tokamaks plasma densities and the O- and X-modes are more weakly coupled, as STELEC shows, and the ray tracing method still can be used in rare plasma. However full wave code modelling is an important at middle and high densities near of X- and O-modes cut offs, to describe the interplay of refraction, reflection, interference and diffraction effects.

2.1 Second Harmonic ECH Scenarios in T-10

Second harmonic X-mode launch in T-10 is shown in FIG.11a: $|real(E_{\psi})|$, at $N=90$ ($N_{\parallel}(0)=0.02$), $F=140$ GHz, $N_e(0)=4.5 \times 10^{19} \text{ m}^{-3}$, $T_e(0)=8.7$ kV, ($\alpha_n=1$, $\alpha_T=2$), $B_0=2.5$ T, $I_p=300$ kA (relativistic effects are included) and power deposition is displayed in the FIG.11b. At plasma increased density $N_e(0)=9 \times 10^{19} \text{ m}^{-3}$ the diffraction is more strong one (FIGs.12a,b). Insert in FIG.12b shows 2D power deposition to the electrons.

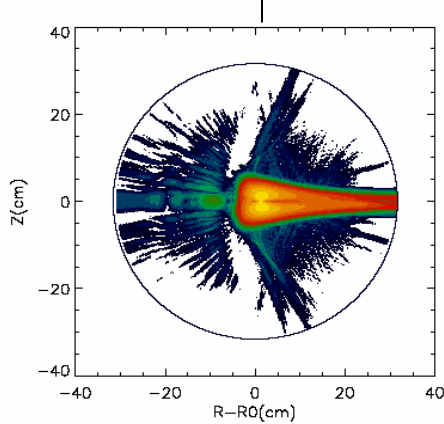


FIG.11a $|real(E_{\psi})|$ in T-10, $N_e(0)=4.5 \times 10^{19} \text{ m}^{-3}$
 $F=140\text{GHz}$

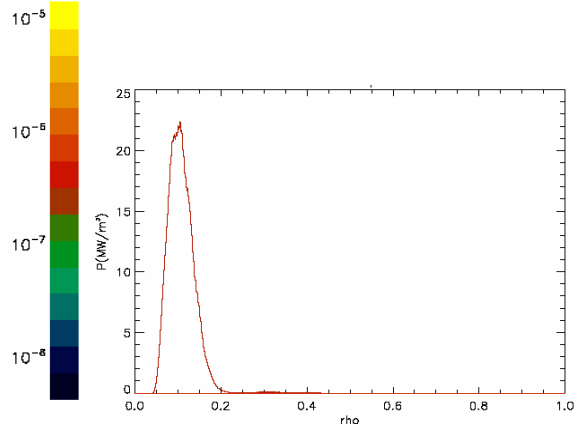


FIG.11b $P_e(\rho)$ in T-10, $\omega = 2\omega_{ce}$,

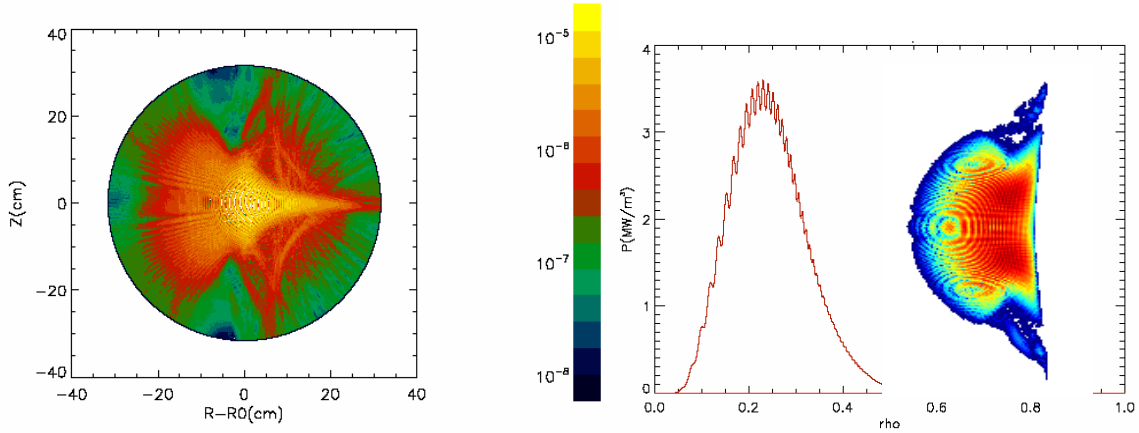


FIG.12a $|real(E_{\psi})|$ in T-10, $N_e(0)=9 \times 10^{19} m^{-3}$ $F=140$ GHz, $N_{||}(0)=0.02$ FIG.12b 1D and 2D P_e in T-10, $N_e=9 \times 10^{19} m^{-3}$ $F=140$ GHz, $N_{||}(0)=0.02$

2.2 Second Harmonic high density ECH Scenarios in JET

We will consider the example for JET ECH second harmonic X-mode outside $F=27.5$ GHz equatorial oblique launch to over dense L-mode plasma: $N(0)=5 \times 10^{18} m^{-3}$, $T_e(0)=9.8$ keV, $N_{||}(0)=0.2$, displayed in FIGs.13a,b for $|E_{\psi}|$ and $|Im(E_z)|$ e.m. field components. FIG.11a shows the X-mode cut off with following wave bouncing in poloidal direction between X-cut off layer and the wall, while simultaneously excited O-mode well focalised beam pattern is propagating to the second harmonic layer near magnetic axis, FIG.13b, not experiencing O-mode cut off. Respective radial power deposition is given in FIG.14.

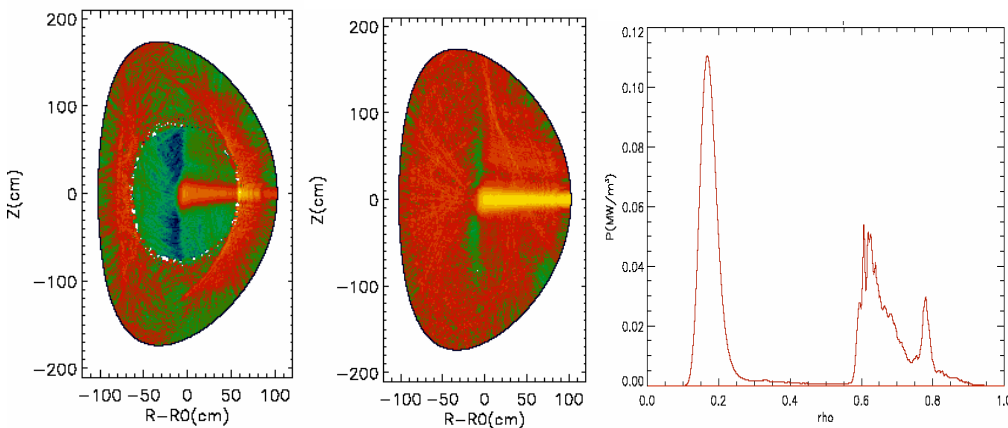


FIG.13a $|Re(E_{\psi})|$ in JET FIG.13b $|Im(E_z)|$ in JET FIG.14 Power deposition in JET

Thus we see a possibility of double peaks power deposition with a single gyrotron frequency. This scenario is a possible candidate for recent AUG ECH high density H-mode scenario with tungsten wall to control impurity accumulation in plasma center [5].

2.3. O-X-B second harmonic scenario in TCV

The O-X-B scenario for over dense plasma at the second harmonic O-mode outside oblique equatorial launch at 82.7 GHz was experimentally explored on the TCV [6]. We have modelled this scenario at machine and plasma parameters: $\kappa = 1.95$, $\delta = 0.4$, $N_e(0) = 7 \cdot 10^{19} \text{ m}^{-3}$, $T_{eo} = 0.97 \text{ kV}$, $B_0 = 1.45 \text{ T}$, $I_p = 415 \text{ kA}$, $q(0) = 0.83$, $q(95) = 4.96$, L-mode with parabolic density profile, RF injection with $N_{//} = 0.277$. This density at specified toroidal injection angle ($N_{//} = 0.277$) is approaching to the critical O-mode density but still is a little lower one. Nevertheless, the double mode conversion process O-X-B is accomplished as demonstrated by FIGs.15a,b displaying the contour plots of $|E_{\text{minus}}|$ (FIGs.15a) and $|\text{Re}(E_{\text{psi}})|$ (FIGs.15b) field components. One sees remarkable conversion to the X-mode which experiences clear X-cut off and following conversion to the EBW. Important to observe that efficient MC process to the EBW occurs not around equatorial plane, where O-mode is injected by an antenna, but at near top and bottom plasma locations more closer to the X-cut off surface – plasma itself finds convenient space places to efficiently convert to the EBW. The EBW propagation behaviour closely resembles EB rays propagation – but with important difference: plasma automatically provides each ray by self consistent initial amplitude. Power deposition follows to this picture of the EBW propagating predominantly along vertical second harmonic resonance surface, FIG. 16.

Summary and Conclusions

The 3D STELEC code was used to numerically model the electron cyclotron and electron Bernstein wave heating in several tokamaks and ITER at the fundamental and second harmonic. The following earlier findings [1] were confirmed: 1) O-mode and X-mode coupling in toroidal plasmas at fundamental EC harmonic; 2) Electron Bernstein waves play a crucial role at O-mode antenna polarization (contrary to what is calculated with ray tracing techniques) and leads to a broadening of the EC power deposition profile. The maximum of the power deposition can be shifted compared to usual ray tracing predictions; 3) we have shown the validity of modelling the fundamental harmonic O-mode scenario for ITER at reduced frequencies, making use of similarity laws [7]; 4) The modelling shows that mode converted EB waves can be generated in the plasma with large amplitudes for the electric field. This could provide a possibility for sheared flow generation ($\sim E^2$), important for ITB creation and plasma turbulence control. It would be therefore be interesting to verify this preliminary conclusion from our modelling work by dedicated experiments. The poloidal magnetic field plays an essential role in the damping of the EB wave on electrons, optimal for flow drive.

Second harmonic X mode scenarios in T-10, DIII-D, TCV and ITER clearly show broader power deposition profiles compared to usual ray tracing results at moderate plasma densities. At low densities the ray tracing approach still works. Refraction and diffraction effects in low and high density plasmas were modelled for circular T-10 and elongated DIII-D tokamaks.

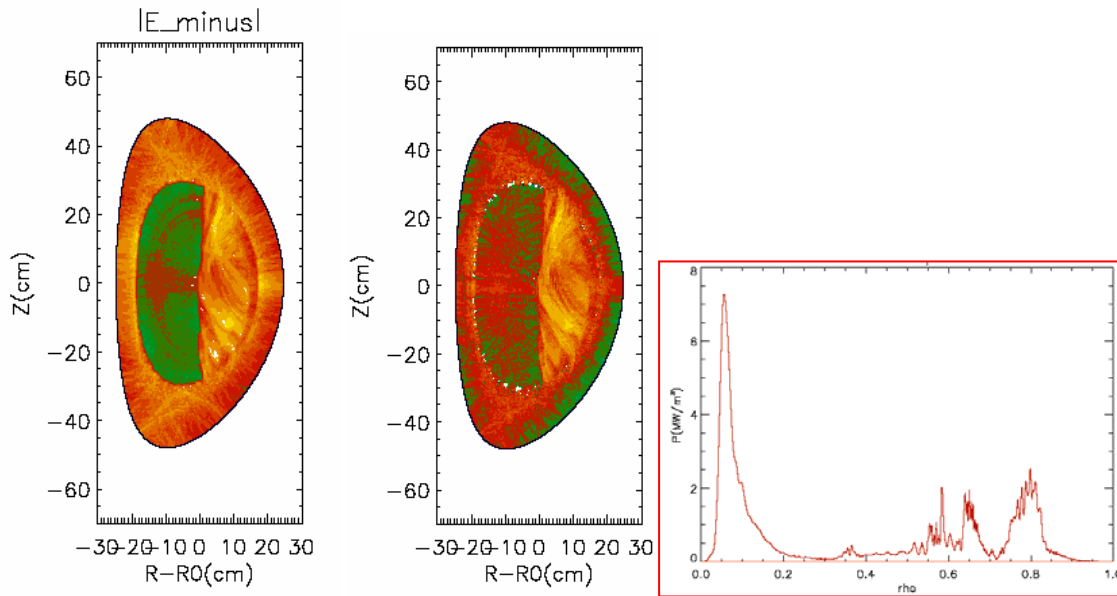


FIG.15 a,b Contour plots of $|E_{\text{minus}}|$ and $|Re(E_{\text{psi}})|$ profile in TCV at 2nd harmonic O-X-B scenario at 82.7 GHz. FIG.16 Radial power deposition for TCV O-X-B scenario

Recent STELEC code modelling for the non active ITER phase in the frequency range 5 – 30 GHz confirmed the validity of using similarity laws to model wave propagation and deposition at reduced frequencies in large fusion machines. The 3D full wave code has shown itself to be a very powerful tool to model ECH and ECCD for many scenarios in toroidal plasmas including O-X-B schemes.

References

1. VDOVIN, V.L. Role of Upper Hybrid resonance and diffraction effects at Electron Cyclotron Heating in tokamaks, Proceedings of EC and ECE 14th Joint Workshop, invited lecture, p.323-333 (Santorini 2006, Greece)
2. PODOBA, Yu. Radio frequency heating on the WEGA stellarator, PHD thesis, Ernst-Moritz-Arndt-Universität Greifswald. 2006
3. PRATER, R. et al, Proc. 7th Top. Conf. Radio Frequency Power in Plasmas, Kissimmee, Florida, 1987, p.9 (American Institute of Physics, 1987)
4. HSU, J.-Y. MOELLER, C.P., in Proc. 7th Top. Conf. Radio Frequency Power in Plasmas, Kissimmee, Florida, 1987, p. 13 (American Institute of Physics, 1987)
5. STOBER, J. et al, Effects of co- and counter-ECCD on improved H-modes in ASDEX Upgrade and implications for the launchers in ITER, ITPA IOS group meeting in NAKA (Japan, April 2009)
6. POCHELON, A., MUECK, CAMENEN, Y. et al, Electron Bernstein Wave Heating of Overdense H-mode Plasmas in the TCV Tokamak via O-X-B Double Mode Conversion, FEC 2008 (Swiss), EX/P6-2
7. VDOVIN, V.L. Electron Cyclotron over dense Plasma Heating modelling with full wave code in Spherical tokamaks, Proceedings of EC and ECE 15th Joint Workshop (Yosemite 2008, USA)